

Investigation of thermomodulation optical spectrum and electronic structure of niobium

A. I. Golovashkin and A. L. Shelekhov

P. N. Lebedev Physics Institute, USSR Academy of Sciences

(Submitted 12 July 1982)

Zh. Eksp. Teor. Fiz **84**, 2141–2152 (June 1983)

The thermomodulation spectra (TMS) of niobium samples with various electron mean free paths are measured in the 0.5 to 3.1 eV region. A dependence of the TMS on the quality of the sample is observed and is due to broadening of the electron state density peak near the Fermi energy. A TMS model based on Bragg interband transitions is proposed. The model describes satisfactorily the main structure of the spectra. A number of electron characteristics of niobium is determined and their dependence on the electron mean free path is found. The TMS fine structure is found.

PACS numbers: 78.20.Nv, 71.25.Pi

INTRODUCTION

Study of the electronic structure of metals and alloys and of its temperature dependence, and of the influence of the electron mean free path, is important for the solution of a large number of problems, particularly high-temperature superconductivity. Valuable information on the electronic structure of a material and on the influence exerted on it by various factors can be obtained by measuring the optical thermomodulation spectrum (TMS).¹ Although recently this procedure came into use for transition metals,^{2–4} the number of such studies is quite limited.

In one of the most interesting regions of the spectrum, that of interband Bragg transitions,^{5,6} the TMS can yield the characteristics of the transitions themselves as well as of the conduction electrons. Modulation procedure, having a high resolving power, makes it possible to investigate also the fine structure of spectra.

In the present paper we study the TMS of niobium samples with different electron mean free paths l , and determine a number of its electron characteristics and their dependence on l . Although the optical properties of Nb were investigated in a number of experimental studies,^{2–4,7–9} and its band structure was calculated in Refs. 10–15, there are no exact answers to many questions connected with the electronic structure of niobium. We do not know the temperature dependences of the band structure, the dependence of the electronic characteristics on l . It appears that the modulation procedure is the optimal optical procedure for the study of such effects.

EXPERIMENTAL DATA

The samples were polycrystalline films obtained by evaporating Nb with an electron beam in a vacuum $(3–5) \cdot 10^{-6}$ torr and by depositing it on polished ruby substrates heated to temperatures $T = 700–900$ °C. The optimal film thickness was 0.3–0.4 μm . This thickness was sufficient to obtain niobium with a fully formed structure and at the same time ensured reasonable values of the currents that modulate the sample temperature during the TMS measurement. By varying the film preparation regime (substrate temperature during the evaporation time, rate of deposition of the film, etc.)

it was possible to obtain niobium samples containing an increase amount of defect. These samples, having decreased electron mean free paths had lower superconducting-transition temperatures T_c and higher resistivities. The parameters of the typical samples for which the TMS were measured are less than in Table I. T_c was measured accurate to 0.1 K, and the accuracy of the measurement of the resistivity was determined by the accuracy of the measurement of the film thickness d and amounted to 7–10%.

The thermal modulation optical spectrum is the frequency-dependent logarithmic derivative of the sample reflection coefficient R with respect to temperature

$$\beta(\omega) = d \ln R / dT \approx (\Delta R / R) \Delta T^{-1},$$

where ΔR is the change of the coefficient of light reflection by the sample due to change in temperature ΔT . The temperature of the samples was modulated by a pulsed current of frequency 23 Hz, which was fed to the Nb film through indium contacts on conducting silver paste. Sample temperature during the time of recording of the modulation signal, and also the depth of the temperature modulation ΔT , were measured with a special bridge circuit.¹⁶ The temperature modulation ranged from 1.5 to 6 K. To maintain the average sample temperature in the course of the experiment at the level 20–25 °C, water cooling was used. Measurement of ΔT yielded the absolute values of the TMS in units of deg^{-1} .

The measurements were performed with the experimental setup of Ref. 16 in the spectral interval 0.5–3.1 eV. To improve the signal noise ratio in the apparatus, multiple accumulation (summation) of the measured signal in the memory of a multichannel analyzer was used; this improved the signal/noise ratio by a factor $n^{1/2}$, where n is the number of

TABLE I.

Sample No.	Thickness, μm	Resistivity, $\mu\text{Ohm-cm}$	T_c , K
1	0.35	22	9.2
2	0.42	31	9.1
3	0.30	39	8.2

summed records of the investigated spectrum. The modulation signal proportional to ΔR , was amplified after leaving the photoreceiver with a tuned amplifier (at the sample-temperature modulation frequency), detected, converted, and recorded in digital form as a function of a wavelength (or ω) in the memory channels of the analyzer. When measuring the spectral dependence of the modulation signal, several hundred records were summed. The signal, proportional to a coefficient of light reflection by the sample, was shaped and measured by the same optical and measuring channels, and the modulation of the light flux was effected by a mechanical chopper at a frequency 1 kHz. The difference in the gains and in the number of records of each signal was taken into account in the subsequent reduction of the experimental data with a computer. Several measurement runs were made for each sample. The final accuracy with which was determined was on the average $(1-2) \cdot 10^{-6} \text{ deg}^{-1}$. The positions of the singularities in the spectra were recorded accurate to 0.01 eV.

MODULATION SPECTRA

Figure 1 shows the TMS of three Nb samples. All the plots have the typical shape of thermomodulation spectra and indicate the complex structure of the spectra. The shapes of all the curves points to the presence, in the interval 0.5–3 eV, of two fundamental bands of interband absorption (the presence of the second band at curve 1 follows from the asymmetry, while at curves 2 and 3 both bands are explicitly manifested), the first at 1.5–1.7 eV and the second at 2–2.1 eV. From these data it follows also that there exists in Nb a third band at $\hbar\omega > 3 \text{ eV}$. In sample No. 3, which contains a larger number of defects, the third band is shifted toward $\hbar\omega \approx 3 \text{ eV}$. The bands 1 and 2 are separated by 0.5–0.6 eV. In the best sample (having the maximum value of T_c) there appears distinctly a fine structure of the spectrum, and the position of the maxima of the fine-structure bands correspond

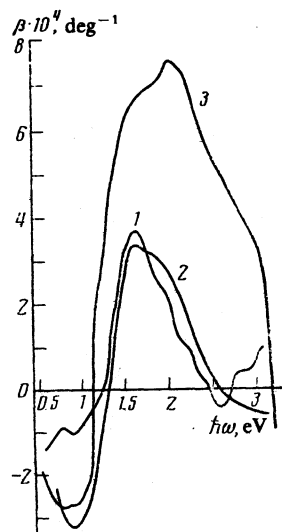


FIG. 1. Thermomodulation spectra of three Nb samples (the numbers of the samples are marked near the curves).

to 0.8, 1.05, 1.5, 2.0, 2.25, and 3.0 eV. There is also a weak singularity in the region 1.5–2.5 eV.

From a comparison of the general form of a spectra of the three samples follows a distinct dependence on the sample quality. First, the value of β at the maximum increases considerably when the quality of the sample deteriorates. The total swing of the β spectrum in the region of the fundamental bands amounts to $5 \cdot 10^{-4} \text{ deg}^{-1}$, $6.5 \cdot 10^{-4} \text{ deg}^{-1}$, and $1 \cdot 10^{-3} \text{ deg}^{-1}$ for samples 1, 2, and 3, respectively. Second, the fine structure is observed only in the best sample and becomes smeared out in the others. In addition, a change is observed in the relative intensity of the different bands on going from sample to sample. Unfortunately, detailed investigations of the thermomodulation spectra of Nb are not available. In Ref. 2 was obtained a TMS in a narrower spectral interval, for example whose quality was not determined. In Refs. 3 and 4, the β spectra of Nb were obtained in relative units. A qualitative comparison of our TMS with the results of Refs. 3 and 4 shows that the spectra agree in general form. The position of the maxima of β coincides in this case with accuracy better than 5%. In Ref. 4, where the properties of bulky samples were measured, just as in our case, a double band was observed in the region 1.5–2.5 eV, as well as a fine structure.

SHAPE OF SPECTRA

To describe the fundamental bands of the TMS of niobium and to determine the electronic characteristics, we used a model based on Bragg interband transitions.^{6,17} It is based on the pseudopotential method, which is successfully used to calculate the electronic structure of transition metals and alloys.^{14,18}

The thermomodulation spectrum β is determined by the contribution made both by interband transitions and by intraband (Drude) absorption. The approximation in which the complex dielectric constant is additive

$$\begin{aligned} \epsilon' &= \epsilon_1 + i\epsilon_2 = 1 + \epsilon_e' + \epsilon_b', \\ R &= \frac{1 + \epsilon - 2^{1/2}(\epsilon + \epsilon_1)^{1/2}}{1 + \epsilon + 2^{1/2}(\epsilon + \epsilon_1)^{1/2}}, \quad \epsilon = (\epsilon_1^2 + \epsilon_2^2)^{1/2}. \end{aligned}$$

The contribution from the conduction electrons ϵ_e' in the case of a weakly normal skin effect¹⁹ can be calculated from the formulas

$$\begin{aligned} \epsilon_e &= \text{Re } \epsilon_e' = -\frac{4\pi e^2 N_e}{m(\omega^2 + \nu_e^2)} (1 - B_1), \\ \sigma_e &= -\frac{\omega}{4\pi} \text{Im } \epsilon_e' = \frac{e^2 N_e \nu_e}{m(\omega^2 + \nu_e^2)} (1 - B_2), \end{aligned}$$

where the correction terms (in the case of the normal skin effect $B_1 \approx B_2 \approx 0$)

$$\begin{aligned} B_1 &= \gamma_1 - \frac{\nu_e}{\omega} \gamma_2, \quad B_2 = \gamma_1 + \frac{\omega}{\nu_e} \gamma_2, \\ \gamma_1 &= \frac{3}{8} \frac{v_F}{c} \frac{\kappa_0}{1 + \nu_e^2/\omega^2} \left(\frac{n_0}{\kappa_0} + \frac{\nu_e}{\omega} \right), \\ \gamma_2 &= \frac{3}{8} \frac{v_F}{c} \frac{\kappa_0}{1 + \nu_e^2/\omega^2} \left(\frac{n_0 \nu_e}{\kappa_0 \omega} - 1 \right), \end{aligned}$$

$$n_0 = \left(\frac{2\pi e^2 N_e}{m(\omega^2 + \nu_e^2)} \right)^{1/2} (-1 + (1 + \nu_e^2/\omega^2)^{1/2})^{1/2},$$

$$\kappa_0 = \left(\frac{2\pi e^2 N_e}{m(\omega^2 + \nu_e^2)} \right)^{1/2} (1 + (1 + \nu_e^2/\omega^2)^{1/2})^{1/2}.$$

Here e and m are the charge and mass of the electron, c is the speed of light, ω is the cyclic frequency of the light, N_e is the conduction-electron density, ν_e is the effective frequency of the conduction-electron collisions, and v_F is the average electron velocity on the Fermi surface. Formulas for the correction terms were obtained on the basis of the use of the results of Ref. 19. The obtained values of the correction terms B_1 and B_2 for Nb did not exceed 1–2%. In other metals, their contribution can be more noticeable.

In the investigated model (model with relaxation time) we have for cubic metals²⁰

$$\frac{N_e}{m} = \frac{2}{3(2\pi\hbar)^3} \oint v dS,$$

where the integration is over the Fermi surface, v is the electron velocity on the Fermi surface and depends on the value of the momenta. The quantity N_e/m determines the conductivity and other kinetic characteristics. The difference between this quantity and the corresponding value for a free-electron gas was attributed by us to the difference between N_e and the valence-electron density N_{val} , assuming m to be the mass of the free electron. The average electron velocity v_F and the frequency ν_e are quantities averaged over the Fermi surface. Contributing to ν_e , in principle, are all the possible collisions of electrons with phonon impurity and defects, with one another, etc.

The contribution made to ε' by the interband transitions can be written in the spectrum region of interest to us in the form

$$\varepsilon'_s = \varepsilon_0 + \frac{4e^2}{m} \sum_g \frac{N_g}{\omega_g^2} I_g, \quad (1)$$

where ε_0 is the total contribution from all the interband transitions except the Bragg transitions, $\omega_g = 2V_g/\hbar$ is the absolute value of the Fourier component of the pseudopotential, \hbar is Planck's constant, N_g is the effective density of the electrons that participate in the interband transitions near the plane with index g . The summation is carried out over all the spectra of the Bragg plane. An expression for I_g is obtained in Ref. 6.

The quantities ω_g (i.e., V_g) determine the energy gaps in the electron spectrum⁶, which appear in the form of singularities (absorption bands), on the experimental optical spectra. The quantities N_g determined the intensities of these bands, i.e., are the analog of the "oscillator strength."

It can be shown that the integral I_g in (1) is determined by the expression

$$I_g = I_g(\omega', \nu_g') = \frac{1}{2\pi m V_g} \int_0^\infty K(x; \omega', \nu_g') \frac{S(x)}{(1+x^2)^{3/2}} dx, \quad (2)$$

where $\omega' = \omega/\omega_g$, $\nu_g' = \nu_g/\omega_g$, and ν_g is the frequency of the collisions of the electrons participating in the Bragg interband transitions. The kernel K for not-too-large x is

$$K(x; \omega', \nu_g') = \frac{1}{1+x^2-\Omega^2}, \quad (3)$$

where $\Omega = \omega' + i\nu_g'$. Quantity $S(x)$ is the area of the intersection of the volume bounded by the real Fermi surface with the plane parallel to the Bragg plane with index g and separated from it by a distance $x = p_g(p_g - p)/mV_g$, where p_g is the distance in momentum space from the center of the Γ band to the Bragg plane with index g , and p is the momentum component particular to the Bragg plane g . Contributing to $S(x)$ are only momentum space regions with nonzero combined state density. In the case when the Fermi momentum $p_F > p_g$, the Bragg planes with index $\{g\}$ intersect the Fermi surface and $S(x)$ is determined by the expressions

$$S(x) = \begin{cases} 4\pi m V_g (1+x^2)^{1/2}, & 0 \leq x \leq x_0, \\ \pi \left(2mE_F - p_g^2 - \frac{m^2 V_g^2}{p_g^2} x^2 + 2m V_g (1+x^2)^{1/2} \right), & x_0 \leq x \leq x_F. \end{cases} \quad (4)$$

Here E_F is the Fermi energy,

$$x_0 = \frac{p_g}{mV_g} \left(2mE_F + p_g^2 - 2mV_g \left(1 + \frac{2p_g^2 E_F}{mV_g^2} \right)^{1/2} \right)^{1/2}, \quad (5)$$

$$x_F = p_g^2/mV_g.$$

The point x_F corresponds to the center of the Γ band ($p = 0$). Formally there exists contribution to I_g also at $x > x_F$, but this contribution can in practice always be neglected because of the strong decrease of the integrand.

For the case of practical importance in which the contribution made to (2) and $x > x_0$ can be neglected (i.e., at $x_0 \gg 1$ or at relatively small V_g : $V_g \ll p_g(p_F - p_g)/m$), the real and imaginary parts of the integral I_g are equal to¹⁷

$$I_1 = \text{Re } I_g = \frac{\pi}{[2B(A+B^{1/2})]^{1/2}} + \frac{(\omega')^2 - (\nu_g')^2}{2\omega'\nu_g'} I_2, \quad (6)$$

$$I_2 = \text{Im } I_g = -2\pi\omega'\nu_g' \frac{1-2A-B^{1/2}+[2B(A+B^{1/2})]^{1/2}}{[2B(A+B^{1/2})]^{1/2}(1-2A+B)}, \quad (7)$$

where $A = 1 - (\omega')^2 + (\nu_g')^2$, $B = A^2 + 4(\omega')^2(\nu_g')^2$. These expressions were used to construct the theoretical form of the β spectrum from the known characteristics and to determine the electronic characteristics of niobium from the experimental spectra.

In the case when $p_F < p_g$ and the corresponding Bragg plane does not cross the Fermi surface, expressions (2)–(5) remain in force, the integration in (2) begins with $x = x_0$. The interband transitions connected with such a plane will lead to noticeable singularities in the spectra when this plane is close enough to the Fermi surface. Characteristic singularities of the spectra, due to such transitions, should be observed at $\omega \approx \omega_g(1+x_0^2)^{1/2}$.

The contribution to the TMS is the result of the temperature dependence of the electronic characteristics V_g and ν_g , as well as of N_e and ν_e . Knowing these dependences and the number of interband-absorption bands, it is possible to construct the theoretical modulation spectrum from the specified electronic characteristics, by using the formulas given above. In principle, it is possible to solve also the in-

verse problem of determining the electronic characteristics from the known TMS.

ELECTRONIC CHARACTERISTICS

The model developed was used to determine the electronic characteristics of Nb from its TMS. The determination of the characteristics was by approximating²¹ the experimental $\beta(\omega)$ dependence with a theoretical curve plotted on the basis of the expressions given above. The calculation algorithm and program, based on the least squares method, are described in detail in Refs. 17 and 22. The parameters varied to fit the theoretical relation to the experimental TMS where $V_g, \nu_g, N_g, N_e, \nu_e$, and the coefficient K_N of the temperature dependence of N_e . In the investigated spectral interval, we usually used 100–200 points.

It was assumed that in the interval 0.3–2.5 eV are located two interband-absorption bands. Their identification¹⁷ leads to the conclusion that the band in the region of 1.6 eV (band No. 1) is connected with the transitions near the Bragg planes with indices $\{200\}$, while the band in region 2 eV (band No. 2) is connected with transitions near the planes $\{110\}$. It must be noted that identification of the bands in the case of Nb is carried out only to assess the possibility of regarding them as Bragg bands. For the $\{200\}$ and $\{110\}$ planes, the value of x_0 is larger enough to justify the use of Eqs. (6) and (7). In this case all the quantities that characterize the concrete system of Bragg planes enter only in N_g . This quantity was varied as a parameter.

To take into account the relatively weak influence of the third band, situated at $\hbar\omega \approx 3$ eV, it was assumed that its shape is also described by Eqs. (2)–(5). It is known⁶ that on the side of small ω the Bragg absorption planes have a much stronger frequency dependence and their influence on the optical properties decreases rapidly. In essence, in this case one uses only the fact that threshold absorption, “smeared out” to the extent that the relaxation time is finite, exists.

By applying the procedure described above the experimental data for sample No. 1, it was shown that they are described by a curve with three fundamental absorption bands. The electronic characteristics and the parameters of all three bands were determined. It was found that the maximum of the third band and the spectrum of β should be located at $\hbar\omega = 315$ eV and is equal to $1 \cdot 10^{-4} \text{ deg}^{-1}$. There is no doubt that the investigated spectrum intervals in which the influence of the third band is noticeable is too limited, so that its parameters are determined with low accuracy.

In Ref. 4, the position of the third band corresponds to each $\hbar\omega = 3.85$ eV. For a more accurate assessment of the influence of this band, the experimental TMS of sample No. 1 of our study was supplemented by high-frequency data from Ref. 4 up to 4.5 eV. In this case, inasmuch as in Ref. 4 there are no absolute values of β , the normalization was carried out in accordance with the maximum of the band No. 1. This procedure is justified when account is taken of the fact that the spectra all have a common shape.

The TMS obtained in this manner in the region 0.5–4.5 eV (Fig. 2, points) was used to calculate the electronic characteristics in accordance with the program of Ref. 22. The values of the electronic characteristics are given in Table II. The TMS calculated on the basis of these characteristics using the formulas given is shown in Fig. 2 in the form of a solid line.

Allowance for band No. 3 from Ref. 4 changed the values of V_g obtained from our data by 1–2%. The other characteristics change in this case more strongly (for example, the value of N_e and ν_e changed by 20% and 14%, respectively).

For sample No. 2, the influence of the third band was taken into account in similar fashion, and we used its parameters obtained in the first case. For sample No. 3, in which the third band drops out in the investigated spectral interval, all the parameters were determined on the basis of the ex-

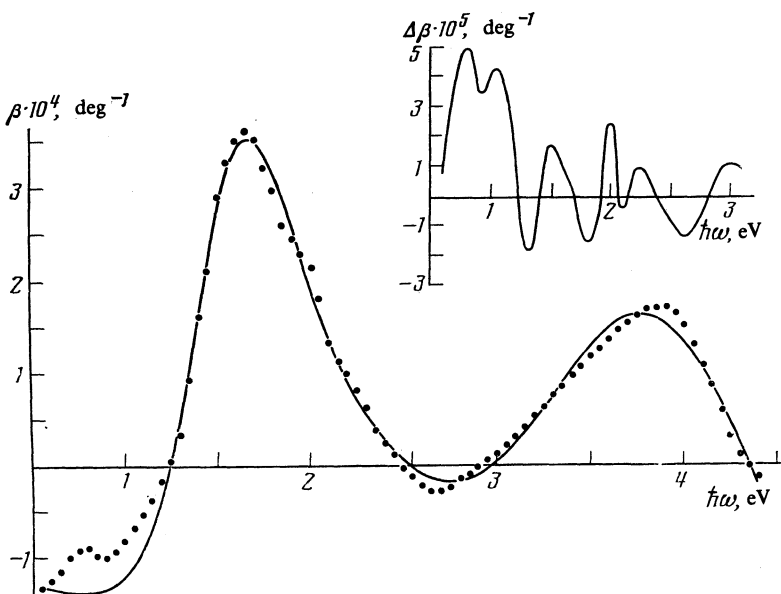


FIG. 2. Thermomodulation spectrum of Nb sample No. 1, supplemented with data from Ref. 4. Solid curve—calculation by the model of Bragg interband transitions with three absorption bands. Inset—spectrum of the quantity $\Delta\beta = \beta_{\text{exp}} - \beta_{\text{theor}}$.

TABLE II.

Sample No.	Band № 1 ($g=\{200\}$)			Band № 2 ($g=\{110\}$)			Conduction electrons		
	V_g, eV	$\nu_g', 10^{15} \text{ s}^{-1}$	$N_g', 10^{22} \text{ cm}^{-3}$	V_g, eV	$\nu_g', 10^{15} \text{ s}^{-1}$	$N_g', 10^{22} \text{ cm}^{-3}$	$N_e, 10^{22} \text{ cm}^{-3}$	$\nu_e', 10^{15} \text{ s}^{-1}$	$K_N, 10^{-4} \text{ deg}^{-1}$
1	0.80	1.1	2.8	1.08	2.3	3.7	5.5	0.5	2.4
2	0.77	0.6	1.7	1.04	0.9	3.7	6.0	0.4	2.6
3	0.73	0.4	1.2	0.94	0.8	1.5	7.4	0.7	15.5

perimental TMS. The characteristics of these samples are also given in Table II.

The error in these characteristics, which was calculated from the formulas of Refs. 17 and 21, amounted to 1–2% for the parameters of bands No. 1 and No. 2, 4% for the values of N_e and ν_0 , and 1% for K_N . In fact, the accuracy of all the quantities is determined by the accuracy of the model of the Bragg interband transition (of the order of V_g/E_F).

The obtained characteristics enable us to calculate the spectral dependences of the optical constants and other optical quantities of niobium. Figure 3 shows the calculated spectrum of the optical conductivity σ ,

$$\sigma = \sigma_e - \frac{e^2 \omega}{m\pi} \sum_g \frac{N_g}{\omega_g^2} I_2$$

for sample No. 1 (solid line). The dashed line shows the contribution from the interband transitions, while the dash-dot line shows the contribution from each band. In Fig. 4 is compared the experimental spectrum σ of Ref. 9 with the calculated spectrum of Nb. It can be seen that not only the general shape of the spectra and the positions of the singularities coincide, but that there is quite good agreement of the absolute values of σ in the region of the Bragg interband transi-

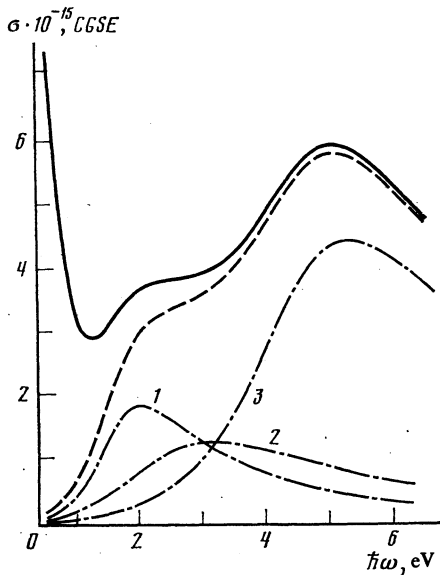


FIG. 3. Spectrum of optical conductivity of niobium, calculated on the basis of characteristics obtained from TMS (solid curve). Dashed curve—contribution to σ from interband transitions; dash-dot—contribution from individual absorption bands (the numbers are indicated next to the curves).

tions. Taking into account the approximate character of the model, the experimental error, and the error in the calculation of σ parameters, and the differences between the samples, such an agreement should be admitted to be good. A comparison of the contribution of the interband transitions with the corresponding experimental curve, obtained in Ref. 7, also shows them to be in good agreement.

The state density on the Fermi surface $N(0)$ can be obtained from the value of N_e , if the average electron velocity v_F on the Fermi surface is known¹⁷

$$N(0) \approx N_e(0) \frac{N_e}{N_{\text{val}}} \frac{v_0^2}{v_F^2}.$$

Here $N_{\text{val}} = 27.8 \cdot 10^{22} \text{ cm}^{-3}$ is the density of the valence electrons of Nb, $N_0(0) = 0.243 \text{ states/eV}\cdot\text{at}\cdot\text{spin}$ is the density of the states of the free electrons on the Fermi surface, which is a sphere, $v_0 = 2.34 \cdot 10^8 \text{ cm/sec}$ is the velocity of the free electrons on the Fermi surface. Assuming $v_F = 0.62 \cdot 10^8 \text{ cm/sec}$ (Ref. 11), we obtain for sample No. 1, which has the highest E_c , the value $N(0) = 0.68 \text{ state/eV}\cdot\text{at}\cdot\text{spin}$. This value agrees well with the data $N(0) = 0.727 \text{ state/eV}\cdot\text{at}\cdot\text{spin}$ (Ref. 11) and $N(0) = 0.732 \text{ state/eV}\cdot\text{at}\cdot\text{spin}$.¹²

DISCUSSION

1. For the first sample, the value of the effective density of the electrons N_g participating in the interband transitions corresponding to the third band was found to be $15.6 \cdot 10^{22} \text{ sec}^{-3}$. (This value characterizes the intensity of the band or the oscillator strength.) Thus, it can be seen that the sum rule¹⁷

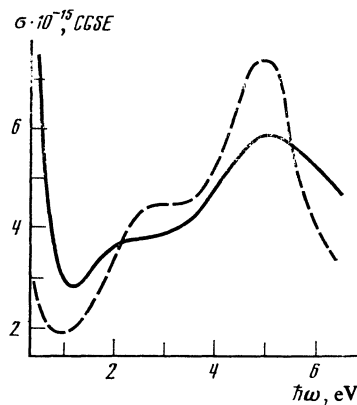


FIG. 4. Comparison of the experimental spectrum from Ref. 9 (dashed curve) with spectrum calculated from the TMS (solid curve).

$$N_{\text{val}} = N_e + \sum_g N_g \quad (8)$$

is splendidly satisfied for this sample. This indicates that there are no other strong bands capable of substantially influencing (8).

If N_e is estimated from Eq. (8) on the basis of the obtained values of N_g , we obtain $N_e = 5.7 \cdot 10^{22} \text{ cm}^{-3}$ for sample No. 1. This agrees well with the quantity $5.5 \cdot 10^{22} \text{ cm}^{-3}$, obtained by direct calculation from the TMS.

If at $\omega \lesssim \omega_p$, where ω_p is the plasma frequency, there exist bands of non-Bragg origin (for example, those connected with transitions from the d or to the d levels), which are characterized by an effective electron density N_d , the sum rule (8) must be written in the form

$$N_{\text{val}} = N_e + \sum_g N_g + \sum_d N_d. \quad (9)$$

The sum over d includes here all the bands of non-Bragg origin.

2. The coefficient of the temperature dependence of N_e is a variable parameter. At the same time, it can be found from (8) by specifying the temperature dependence of V_g . Using for the latter the value $1.2 \cdot 10^{-4} \text{ deg}^{-1}$, obtained on the basis of experimental data,^{3,7} we get $K_N = (1/N_e) dN_e/dT = 1.8 \cdot 10^{-4} \text{ deg}^{-1}$, which is in good agreement with the value $2.4 \cdot 10^{-4} \text{ deg}^{-1}$ (Table II). In Ref. 7, direct experiment (for the temperature interval 78–293 K) yielded $K_N = 1.7 \cdot 10^{-4} \text{ deg}^{-1}$. The agreement of the coefficient K_N , obtained by different methods, as well as the satisfaction of the sum rule (8) or (9) and the satisfactory agreement of the calculated spectrum σ with experiment, offer evidence of sufficiently good description of the optical properties of Nb by the model of Bragg interband transitions. This agreement enables us to obtain, on the basis of the TMS, important electronic characteristics.

3. From the data obtained in the present paper follows a definite dependence of the TMS on the quality of the Nb samples. When the quality of the sample is poor, as is manifested by a decrease of T_c and by an increase of the resistivity ρ , the number of singularities of the TMS in the region of the interband transition band increases, the fine structure vanishes. Similar phenomena were observed earlier in niobium alloys with molybdenum.⁴ With increasing content of Mo in Nb, the value of β at the maximum also increases considerably. This change of the optical properties of niobium can be attributed to smearing of the peak of the electronic state density $N(E)$ near the Fermi level with decreasing electron mean free path l . According to the data of Refs. 11, 18, and 23, one can estimate the width of the peak of $N(E)$ of niobium near E_F at $\delta E \approx 0.5 - 0.7 \text{ eV}$. Thus, at $l \sim \hbar v_F / \delta E \approx 6 - 10 \text{ \AA}$ there should be observed in Nb a strong dependence of $N(E_F)$, meaning also of other electronic characteristics, on l , i.e., on the quality of the sample. At these values of l an additional temperature dependence appears of the electron and optical properties of niobium and is connected with the dependence of l on T . This should lead in particular to enhancement of the singularities of the TMS.

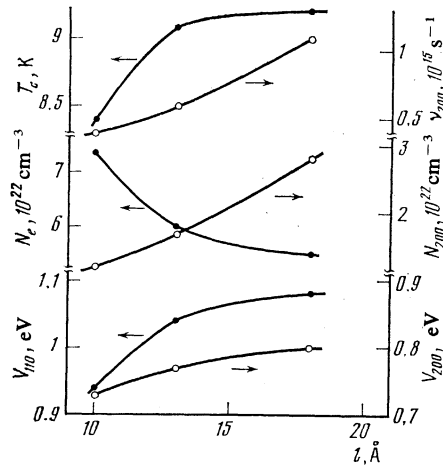


FIG. 5. Dependence of a number of characteristics and of T_c of Nb on the electron mean free path.

An estimate of the value of l in our best sample of Nb from the obtained values of ρ and N_e yields a value 18 \AA (we used the value of V_F indicated above). To estimate l in other samples, it can be assumed in first-order approximation that $l\rho \approx \text{const}$. This approximation was sufficiently well verified in experiment and is connected with the fact that both N_e and v_F increase with decreasing l .²⁴ In this case we obtain $l = 13 \text{ \AA}$ and 10 \AA respective for samples No. 2 and No. 3. It can be seen therefore that effects connected with the smearing of the $N(E)$ peak near E_F are perfectly observable in our samples.

Besides smearing the $N(E)$ peak, an increase of l changes other electronic characteristics, as well as T_c , in Nb. Figure 5 shows the obtained l -dependences of a number of characteristics of Nb. A noticeable change of such characteristics as N_e , V_g , and T_c is observed at $l \approx 10 - 15 \text{ \AA}$. In bulky Nb with $l = 56 \text{ \AA}$, we have $N_e = 4.5 \cdot 10^{22} \text{ cm}^{-3}$ (Ref. 7), in good agreement with the obtained dependence of N_e on l . The observed dependences of V_g on l seem perfectly natural, since the energy smearing at the corresponding relaxation times becomes comparable with V_g values $0.8 - 1 \text{ eV}$. The substantially smaller electric gaps corresponding to the smaller V_g will be completely smeared out at such l .

The observed change of the characteristics with decreasing l agrees with the previously obtained²⁵ correlations of T_c in particular, we note that the correlation of T_c with V_g and N_e , which was observed for different Nb samples.

For samples No. 2 and No. 3 we obtained respectively $v_F = 0.67 \cdot 10^8 \text{ cm/sec}$ and $0.83 \cdot 10^8 \text{ cm/sec}$, $N(0) = 0.63 \text{ state/eV}\cdot\text{at. spin}$ and $0.51 \text{ state/eV}\cdot\text{at. spin}$. The values of their T_c turn out here to be proportional to $N^{1/2}(0)$.

We attribute the change of the electronic characteristics, such as the conduction-electron density of the electronic states on the Fermi surface, the electron velocity on the Fermi surface, and other in our Nb samples with the change of l (or of the electron collision frequency). In principle this should lead to noticeable dependences of these characteristics on the temperature. Unfortunately, no such ex-

periments have been performed to date. We regard as well likely an influence on the characteristics (for example, on N_e) by a change of the impurity content of the samples. The samples were prepared under close conditions and the most substantial parameter that influences T_c , ρ , and l was the substrate temperature during the deposition of the film.

4. The optical constants of niobium were measured earlier⁷ by an ellipsometric method. The shape of the absorption band σ obtained in Ref. 7 in the region 1–3 eV indicates that it has a complicated character and confirms the presence in the region of two fundamental overlapping ends. In Ref. 7 and in the succeeding studies^{26,27} it was assumed that only one of these bands is fundamental. The corresponding values of V_g were found to be 11.8 eV (Ref. 7), 0.89 eV (Ref. 26), and 1.13 eV (Ref. 27). These values must be compared with the value of V_g for the second band of the present paper. If it is assumed that both bands are of the Bragg type in the interval 1–3 eV, we obtain on the basis of the experimental data of Ref. 7 the estimate $V_{g1} = 0.85$ eV and $V_{g2} = 1.25$ eV. These values agree well with those obtained from TMS.

5. In the absence of interband transitions, the plasma frequency in Nb should be, in energy units, $\omega_p = (4\pi e^2 N_e / m)^{1/2} \approx 8.6$ eV for the first sample and 9.1 eV for the second. In the presence of Bragg interband transitions near ω_p , this frequency increases.⁶ If we continue formally the obtained frequency dependence ε_1 into the region of large ω , then, when account is taken of the Bragg transitions, we obtain for sample No. 1 $\omega_p \approx 17.2$ eV and $\omega_p \approx 17.5$ eV for sample No. 2. Using in the expression for ω_p the value $N_e = N_{val}$, we obtain $\omega_p \approx 19.6$ eV.

In Refs. 12 and 13 they obtained respectively $\omega_p = 9.96$ and 8.87 eV. These values are close to our value of ω_p obtained without allowance for the Bragg interband transitions. The absence of or the small contribution from Bragg transitions at $\omega \sim \omega_p$ are perfectly permissible, inasmuch as at high frequencies the approximations on which the model is based are violated. In experiment one observes at such ω a complicated picture. In Ref. 8 two maxima were observed on the bulk-curve at energies 9.5 eV and 19.6 eV, and in Ref. 9, at 8.8 eV and 20.8 eV.

Since the theoretical model accounts for only the basic (Bragg) interband transitions, to reveal the fine structure we constructed the spectrum of the quantity $\Delta\beta = \beta_{exp} - \beta_{theor}$ (inset of Fig. 2). Here β_{exp} is the experimental TMS, and β_{theor} is a spectrum calculated from the electronic characteristics and contains only Bragg bands. The spectrum $\Delta\beta$ is qualitative in character, showing the position of the additional singularities and their relative magnitude. One can see in the figure the complicated structure of the spectrum $\Delta\beta$. The absolute values of the singularities amounts to $(1 - 5) \cdot 10^{-5} \text{ deg}^{-1}$. The spectrum seems to reflect the complicated energy dependence of the density of the electronic states.¹¹ The corresponding interband transitions take place in individual small sections of momentum space and are separated because of the sufficiently strong temperature dependence of their parameters. In Ref. 4 we observed a fine structure of the TMS at 1.38 eV and 2.36 eV; this is in satisfactory agreement with the singularities obtained by us at 1.5 eV, in

the region 2.25–2.5 eV.

7. In the present paper band No. 3 was identified with a Bragg band corresponding to the planes $\{211\}$. Since these planes do not cross the Fermi sphere of the free electrons, the singularities in the spectrum should be observed at $\omega \sim \omega_g (1 + x_0^2)^{1/2}$. At $E_g E_F \gg V_g^2 / 4$ we have $x_0 \approx p_g \times (p_g - p_F) / m V_g$, where $E_g = p_g^2 / 2m$ and $p_F = (2mE_F)^{1/2}$. From the position of the maximum of β of the third band $\hbar\omega_{max} \approx 3.9$ eV we estimate in this case that $V_g \lesssim 1.9$ eV.

In principle, such an interpretation of the absorption band of niobium, located in the region of 4 eV, is not the only one. It is possible that the corresponding transitions are connected with d -levels. In this case the detailed shape of the band changes, reflecting the character of the d -band, but its threshold form, smeared out because of the finite relaxation time, remains. For a final conclusion concerning the nature of the band it is necessary to investigate in detail its shapes and compare them with theoretical models.

In principle, one can consider also other identifications of the observed bands than the one used in the present paper. A substantial change will be consideration of the first two bands as being of non-Bragg origin. Unfortunately, we do not know any models of modulation spectra based on other types of transitions and describing the complete shape of the bands. Apparently one of the interesting critical experiments on the identification of bands will be an experiment on amorphous (or very finely dispersed) niobium.

It is of interest to carry out detailed investigations of the dependence of the optical properties of Nb on the mean free path of the electrons on a larger interval of variation of l . Such investigations, performed for example on samples with a controllable amount of defects produced by irradiation with high-energy particles, will permit an experimental determination of the peak of the state density near the Fermi energy.

In conclusion, the authors thank L. I. Makhshvili for preparing the samples.

¹M. Cardona, Optical Modulation Spectroscopy of Solids, Academic, 1969.

²A. I. Golovashkin, K. V. Mitsen, and G. P. Motulevich, Fiz. Tverd. Tela (Leningrad) **14**, 1704 (1972) [Sov. Phys. Solid State **14**, 1467 (1972)].

³J. H. Weaver, D. W. Lynch, C. H. Culp, and R. Rosei, Phys. Rev. **B14**, 459 (1976).

⁴E. Calavita, A. Franciosi, R. Rosei, F. Sacchetti, E. S. Giuliano, R. Ruggeri, and D. W. Lynch, Phys. Rev. **B20**, 4864 (1979).

⁵W. A. Harrison, Phys. Rev. **147**, 467 (1966).

⁶A. I. Golovashkin and G. P. Motulevich, Zh. Eksp. Teor. Fiz. **57**, 1054 (1969) [Sov. Phys. JETP **30**, 575 (1970)]. FIAN Preprint No. 76, 1969.

⁷A. I. Golovashkin, I. E. Leksina, G. P. Motulevich, and A. A. Shubin, Zh. Eksp. Teor. Fiz. **56**, 51 (1969) [Sov. Phys. JETP **29**, 27 (1969)].

⁸J. H. Weaver, D. W. Lynch, and C. G. Olson, Phys. Rev. **B7**, 4311 (1973).

⁹E. S. Black, D. W. Lynch, and C. G. Olson, Phys. Rev. **B16**, 2337 (1977).

¹⁰R. A. Decgan and W. D. Twose, Phys. Rev. **164**, 993 (1967).

¹¹L. F. Mattheiss, Phys. Rev. **B1**, 373 (1970).

¹²W. E. Pickett and P. B. Allen, Phys. Rev. **B11**, 3599 (1975); **B13**, 1473 (1976).

¹³B. Chakraborty, W. E. Pickett, and P. B. Allen, Phys. Rev. **B14**, 3227 (1976).

¹⁴S. G. Louie, K. M. Ho, J. R. Chelikowsky, and M. L. Cohen, Phys. Rev. **B15**, 5627 (1977).

¹⁵G. Louie, K. M. Ho, and M. L. Cohen, Phys. Rev. **B19**, 1774 (1979).

¹⁶A. I. Golovashkin and A. L. Shelekhov, Prib. Tekh. Eksp. No. 5, 216 (1980). FIAN Preprint No. 71, 1979.

- ¹⁷A. I. Golovashkin and A. L. Shelekhov, *Kratk. Soobshch. Fiz.* No. 5, 11 (1978). FIAN Preprint No. 96, 1981.
- ¹⁸C. Y. Fong and M. L. Cohen, *Phys. Lett.* **44A**, 375 (1973).
- ¹⁹G. P. Motulevich, *Zh. Eksp. Teor. Fiz.* **46**, 287 (1964) [*Sov. Phys. JETP* **19**, 199 (1964)].
- ²⁰G. P. Motulevich, *Usp. Fiz. Nauk* **97**, 211 (1969) [*Sov. Phys. Usp.* **12**, 80 (1969)].
- ²¹T. A. Agekyan, *Osnovy teorii oshibok dlya astronomov i fizikov* (Principles of Error Theory for Astronomers and Physicists), Nauka, 1972.
- ²³N. Elyashar and D. D. Koelling, *Phys. Rev.* **B15**, 3620 (1977).
- ²⁴A. I. Golovashkin, E. V. Pechen', and N. P. Shabanova, *Zh. Eksp. Teor. Fiz.* **82**, 550 (1982) [*Sov. Phys. JETP* **55**, 503 (1982)] FIAN Preprint No. 238, 1981.
- ²⁵A. I. Golovashkin, I. S. Levchenko, and G. P. Motulevich, *Fiz. Tverd. Tela (Leningrad)* **20**, 3061 (1978) [*Sov. Phys. Solid State* **20**, 1764 (1978)].
- ²⁶A. I. Golovashkin and G. P. Motulevich, *Kratk. Soobshch. Fiz.* No. 2, 69 (1970).
- ²⁷I. D. Mash, *Trudy FIAN* **85**, 3 (1975).

Translated by J. G. Adashko